Optics Letters

Surface exciton polaritons supported by a J-aggregate-dye/air interface at room temperature

Kentaro Takatori,[1,2,3] Takayuki Okamoto,[1,4,*] Koji Ishibashi,[1,4] and Ruggero Micheletto[3]

[1]Advanced Device Laboratory, RIKEN, Hirosawa, Wako, Saitama 351-0198, Japan
[2]Interdisciplinary Graduate School of Science and Engineering, Tokyo Institute of Technology, Nagatsuta, Midori-ku, Yokohama, Kanagawa 226-8503, Japan
[3]Graduate School of Nanobioscience, Yokohama City University, Seto, Kanazawa-ku, Yokohama, Kanagawa 236-0027, Japan
[4]RIKEN Center for Emergent Matter Science, Hirosawa, Wako, Saitama 351-0198, Japan
*Corresponding author: okamoto@riken.jp

Received 20 July 2017; revised 31 August 2017; accepted 1 September 2017; posted 6 September 2017 (Doc. ID 302978); published 25 September 2017

Surface exciton polaritons (SEPs) are very important for the realization of novel sensors and next-generation optical devices. Here we propose for the first time, to the best of our knowledge, a Kretschmann–Raether device that is able to induce SEPs propagating along the interface between a J-aggregate cyanine dye and air at room temperature. This configuration has the advantages of being straightforward to realize and easy to study because the Kretschmann–Raether approach is the most simple and fundamental from the theoretical point of view. Here a J-aggregate cyanine dye produces strong binding energy due to Frenkel excitons, and this enables the observation of SEPs easily at room temperature. One of the advantages of the use of the J-aggregate cyanine dye is the simple device preparation. This is because the J-aggregate cyanine dye can be easily deposited on any arbitrary substrates with a spincoating or dip-coating technique from its aqueous solution in ambient condition. We observed SEPs at room temperature, and the deepest resonant peak was obtained for a 94 nm thick 5,6-dichloro-2-[[5,6-dichloro-1-ethyl-3-(4-sulfobutyl)-benzimidazol-2-ylidene]-propenyl]-1-ethyl-3-(4-sulfobutyl)-benzimidazolium hydroxide film at 532 nm wavelength. Our results may pave the way for the realization of novel SEP biosensors in a simple and straightforward way at room temperature.

OCIS codes: (160.4890) Organic materials; (240.0240) Optics at surfaces; (240.5420) Polaritons; (240.6680) Surface plasmons; (260.6970) Total internal reflection.

https://doi.org/10.1364/OL.42.003876

Surface polaritons are surface electromagnetic waves propagating along a surface of a medium whose permittivity is negative due to plasmons, excitons, or phonons. Among them, surface exciton polaritons (SEPs) have been experimentally observed at a surface of various inorganic and organic crystals in previous works [1–5]. The common property of the excitons in these media is their strong oscillation strength, which gives strong coupling to the electric field. Extremely low temperature is required for supporting SEPs in inorganic crystals, because excitons in these media are Wannier–Mott excitons whose binding energy (~0.01 eV) is lower than the thermal energy at room temperature (0.025 eV) [6]. On the other hand, excitons in organic material are Frenkel excitons which have higher binding energy (0.1–1 eV) than the thermal energy at room temperature [6]. Actually, SEPs in organic crystals were observed at room temperature [5]. However, SEPs in non-crystalline media at room temperature have not been reported, to the best of our knowledge. In this Letter, we observe SEPs at the surface of a J-aggregate cyanine dye film as an organic non-crystalline medium.

Cyanine dye easily forms a J-aggregate in polar solvent such as water. In the J-aggregate, the binding energy of the Frenkel excitons is quite high due to the dipole-dipole interaction between molecules. This results in a very narrow redshifted and strong absorption band, called J-band, compared to that in monomers [7–9]. This property realizes strong vacuum Rabi splitting through coupling of the J-aggregate cyanine dye and surface plasmon polaritons [10–12]. Bellessa *et al.* observed strong coupling between surface plasmons and excitons at the interface between silver and cyanine dye [13]. One of the advantages of J-aggregate cyanine dye to support SEPs is the simplicity of the device preparation. J-aggregate cyanine dye can be easily deposited on any arbitrary substrates with spincoating or dip-coating from its aqueous solution in ambient condition.

Figure 1(a) shows the chemical formula of a 5,6-dichloro-2-[[5,6-dichloro-1-ethyl-3-(4-sulfobutyl)-benzimidazol-2-ylidene]-propenyl]-1-ethyl-3-(4-sulfobutyl)-benzimidazolium hydroxide (TDBC) molecule, which is the cyanine dye we used. Although TDBC is partially crystalline, it can be easily deposited with spincoating or dip-coating. First, we measured the thickness and the complex dielectric constant of a TDBC film. For the thickness measurement, we modified the surface of a 1 mm thick glass substrate by depositing a polyvinyl alcohol (PVA) and a silica film, whose total thickness was 25 nm [see Fig. 1(b)], because it is difficult to peel off the sticky TDBC film which

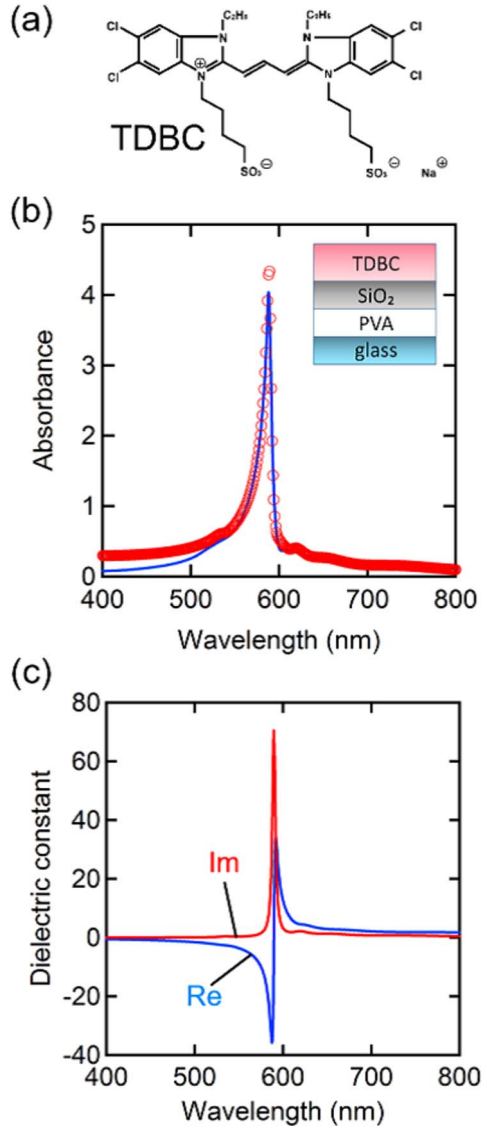

Fig. 1. (a) Chemical formula of TDBC. (b) Measured (solid curve) and fitted (circles) absorption spectra of a 60 nm thick TDBC film on 25 nm thick silica/PVA composite film and glass substrate at room temperature. The inset shows the structure of the sample. (c) Calculated complex dielectric constant of the TDBC film via fitting.

is directly deposited on a glass substrate. This process is required to measure the thickness of the film with an atomic force microscope (AFM). The PVA layer between the TDBC film and the glass substrate makes it easy to peel off the TDBC/silica/PVA composite film from the glass substrate. The surface of the silica layer gives the same condition as that of the glass substrate in the spincoating process. We spun a 30 mM TDBC aqueous solution on this substrate, then peeled off a part of the film and measured the step height by an AFM (VN-8010, Keyence). The obtained thickness of the TDBC film was 60 nm. Figure 1(b) shows the absorption spectrum of the same sample measured with a UV-Vis spectrophotometer (UV-2550, Shimadzu). The absorption peak at 588 nm represents the characteristics of the J-aggregate, whereas the absorption peak for monomers may

Table 1. Fitted Parameters

j	ω_{pj} (cm^{-1})	ω_{0j} (cm^{-1})	γ_j (cm^{-1})
1	4340	13,570	2409
2	4383	15,330	1352
3	3511	16,140	565.5
4	11830	16,960	117.3
5	1621	18,710	561.6

appear at ~530 nm [9]. We calculated the dielectric constant of the TDBC film by fitting a model consisting of five Lorentzian oscillators:

$$\epsilon(\omega) = \epsilon_\infty + \sum_{j=1}^{5} \frac{\omega_{pj}^2}{\omega_{0j}^2 - \omega^2 - i\gamma_j\omega}, \tag{1}$$

to the observed spectrum. In the fitting we ignored the silica/PVA layers since they have almost the same refractive index as the glass substrate in the measurement wavelength region. Table 1 summarizes the fitted parameters. Figure 1(c) shows the estimated real and imaginary part of the dielectric constant of the TDBC film, and the best fitting was given with $\epsilon_\infty = 0$. To have SEPs on the TDBC film, the real part of the dielectric constant should be less than −1. Thus, as shown in Fig. 1(c), the TDBC surface actually supports SEPs in the range from 463 to 589 nm.

Next, we observed SEPs using the Kretschmann–Raether configuration [14], where the metal film was replaced with a TDBC film, as shown in Fig. 2. A glass substrate, of which one surface was deposited with a TDBC film, was attached to the bottom surface of a BK7 prism ($n = 1.52$) using index matching oil. We measured the reflection intensity as a function of the angle of incidence. A 532 nm wavelength laser beam (125 mW, GREEN-SLM LASER, Uniphase) with p-polarization was used as the incident light. All measurements were done at room temperature. Figure 3(a) shows the measured reflection curves for the TDBC films with several thicknesses. The reflection curves were normalized to the maximum intensity. Each reflection curve exhibits a resonant dip derived from SEP resonance at an angle of ~50°, which is larger than the critical angle for the interface of the prism and air. The depth of the resonance dip initially increases and then decreases with the thickness of the TDBC film. The deepest dip was obtained for a 94 nm thick TDBC film at 53.6°.

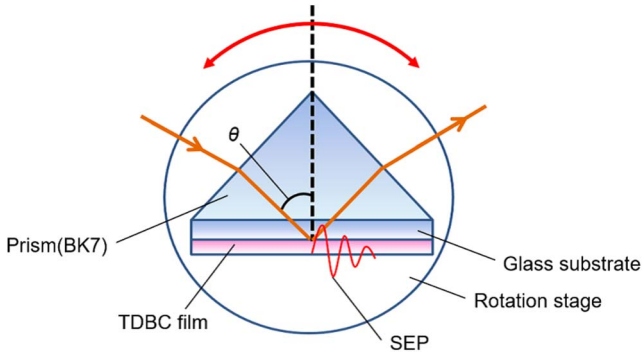

Fig. 2. Experimental arrangement for the attenuated total reflection (ATR) measurement.

We calculated reflectance as a function of the angle of incidence using the dielectric function shown in Fig. 1(c) for the same configuration as the experiment. Figure 3(b) shows calculated reflection curves for TDBC films with several thicknesses. In this calculation, we used a fitted dielectric constant $\epsilon = -2.59 + 0.375i$. The deepest dip was obtained for a 60 nm thick TDBC film at 54.7°. The width of the calculated dips was much narrower than that of the experimental results. Two reasons can be considered for the broadening of the dip width in the experiments. One is the surface roughness of the TDBC films, and the other is the thickness inhomogeneity in those films. The measured root-mean-square roughness of the TDBC films was 6.4–9.9 nm. The surface roughness in the TDBC films causes the scattering of SEPs. This scattering shortens the propagation length of SEPs, resulting in the broadening of the dip's width [14]. The large thickness inhomogeneity also broadens the resonant dip width, since the resonant angle depends on the thickness of the TDBC film in the Kretschmann–Raether configuration. In this case, the dip becomes shallower, because the reflectance curve is given by the average of those that correspond to each thickness. However, the experimental spectrum for the 94 nm thick film showed almost zero reflectance at the dip. For this reason, we concluded that the broadening of the dip width was mainly caused by the surface roughness of the TDBC films.

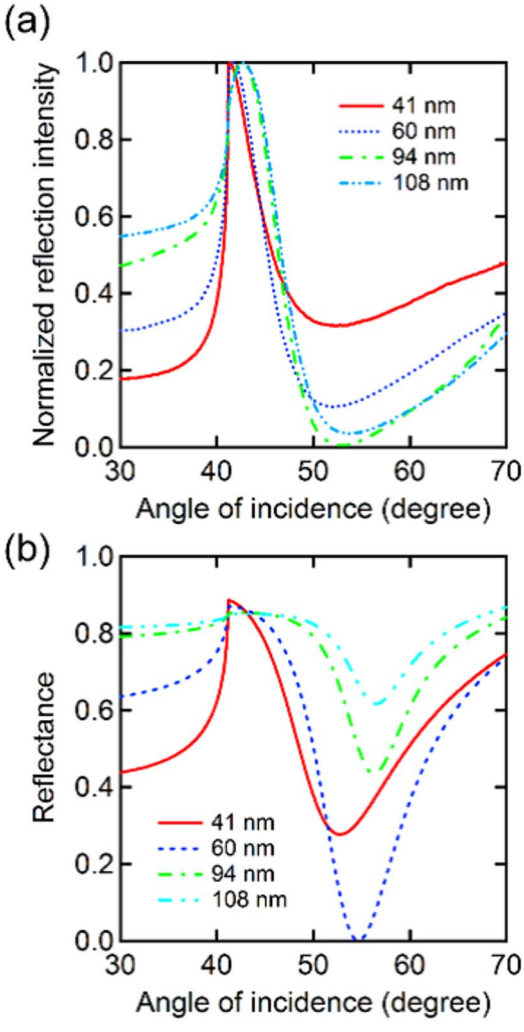

Fig. 3. (a) Experimental and (b) calculated ATR reflection of 41, 60, 94, and 108 nm thick TDBC films.

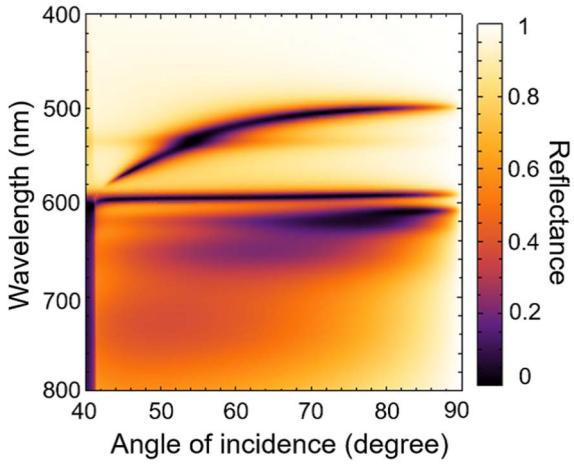

Fig. 4. Calculated dispersion relation of an SEP at the interface between a TDBC film and air in the Kretschmann–Raether configuration.

Figure 4 shows the dispersion relation of the SEP in the Kretschmann–Raether configuration shown in Fig. 2, calculated with the dielectric function of TDBC shown in Fig. 1(c). The reflectance is mapped as a function of wavelength and the angle of incidence. The assumed thickness of the TDBC film was 60 nm. The locus of the reflection minimum in the wavelength region shorter than 580 nm corresponds to the dispersion relation of the SEP.

An interesting phenomenon can be seen in the behavior of the resonance curves for SEPs, when it is compared to surface plasmon polaritons in silver, gold, or aluminum in the Kretschmann–Raether configuration. It is well known that the resonant angle shifts toward a smaller angle as the thickness of the metal film increases [14]; in contrast, in our case, the resonant angle shifts toward larger angles with thickness. We calculated reflectance spectra in the Kretschmann–Raether configuration with several combinations of the real part and the imaginary part of the dielectric constant of the thin film to investigate this phenomenon. We noticed that when the absolute value of the real part is relatively small, the resonant angle shifted toward larger angles as the thickness of the film increases, whereas when the value is relatively large, the resonant angle shifted toward smaller angles. We discovered that the direction of the angular shift changed at $|\mathrm{Re}(\epsilon)| \sim 5$, when the dielectric is air. The absolute value of the real part of the dielectric constant of TDBC films is $|\mathrm{Re}(\epsilon)| = 2.59$ at 532 nm, which is much smaller than that for silver, gold, and aluminum.

In conclusion, we obtained for the first time, to the best of our knowledge, a J-aggregate cyanine dye that is able to realize SEPs at room temperature. In addition, we obtained the dielectric function of the TDBC film by fitting a Lorentzian model to the absorption spectrum of the TDBC/silica/PVA film. From this function, we were able to understand that SEPs can be supported by the TDBC films in the wavelength region starting from 463 to 589 nm. We used the Kretschmann–Raether configuration on the TDBC organic non-crystalline medium at

room temperature. We observed SEPs on this surface and obtained the deepest resonant dip for the 94 nm film thickness at an incident angle of 53.6°, when excited at a wavelength of 532 nm. The observed dip width was broader than the calculated one because of the scattering loss due to the surface roughness of the TDBC film. Nevertheless, the results demonstrate the existence of SEPs at room temperature with our J-aggregate cyanine dye system. This may have implications for the realization of novel SEP-based biosensors or optical devices. There are additional potential advantages of the use of organic materials, such as the possibility to synthesize novel molecules with less damping and the possibility to pattern such active materials with more ease than using metals, with better versatility in the functionalization/linking of molecules. Moreover, organic excitonic materials have substantial optical nonlinearity, which could be exploited for novel sensors or devices [15–18].

Acknowledgment. A part of this Letter was supported by the RIKEN Junior Research Associate Program.

REFERENCES

1. J. Lagois and B. Fischer, Phys. Rev. Lett. **36**, 680 (1976).
2. I. Hirabayashi, T. Koda, Y. Tokura, J. Murata, and Y. Kaneko, J. Phys. Soc. Jpn. **40**, 1215 (1976).
3. I. Hirabayashi, T. Koda, Y. Tokura, J. Murata, and Y. Kaneko, J. Phys. Soc. Jpn. **43**, 173 (1977).
4. Y. Tokura, T. Koda, I. Hirabayashi, and S. Nakada, J. Phys. Soc. Jpn. **50**, 145 (1981).
5. K. Tomioka, M. G. Sceats, and S. A. Rice, J. Chem. Phys. **66**, 2984 (1977).
6. S. Kéna-Cohen and S. R. Forrest, Nat. Photonics **4**, 371 (2010).
7. D. G. Lidzey, D. D. C. Bradley, M. S. Skolnick, T. Virgili, S. Walker, and D. M. Whittaker, Nature **395**, 53 (1998).
8. P. A. Hobson, W. L. Barnes, D. G. Lidzey, G. A. Gehring, D. M. Whittaker, M. S. Skolnick, and S. Walker, Appl. Phys. Lett. **81**, 3519 (2002).
9. J. Moll, S. Daehne, J. R. Durrant, and D. A. Wiersma, J. Chem. Phys. **102**, 6362 (1995).
10. I. Pockrand, A. Brillante, and D. Möbius, J. Chem. Phys. **77**, 6289 (1982).
11. J. Dintinger, S. Klein, F. Bustos, W. L. Barnes, and T. W. Ebbesen, Phys. Rev. B **71**, 035424 (2005).
12. C. Bonnand, J. Bellessa, and J. C. Plenet, Phys. Rev. B **73**, 245330 (2006).
13. J. Bellessa, C. Bonnand, and J. C. Plenet, Phys. Rev. Lett. **93**, 036404 (2004).
14. H. Raether, *Surface Plasmons on Smooth and Rough Surfaces and on Gratings* (Springer, 1988).
15. R. Naraoka, H. Okawa, K. Hashimoto, and K. Kajikawa, Opt. Commun. **248**, 249 (2005).
16. S. S. Lampoura, C. Spitz, S. Dähne, J. Knoester, and K. Duppen, J. Phys. Chem. B **106**, 3103 (2002).
17. A. Pugžlys, P. R. Hania, C. Dodraga, J. Knoester, and K. Duppen, Solid State Phenom. **97–98**, 201 (2004).
18. G. Lerario, D. Ballarini, A. Fieramosca, A. Cannavale, A. Genco, F. Mangione, S. Gambino, L. Dominici, M. De Giorgi, G. Gigli, and D. Sanvitto, Light Sci. Appl. **6**, e16212 (2017).